Experimental Verification of a New Mechanism for Dissociative Chemisorption: Atom Abstraction

Y. L. Li, D. P. Pullman, J. J. Yang, A. A. Tsekouras, D. B. Gosalvez, K. B. Laughlin, Z. Zhang, M. T. Schulberg, D. J. Gladstone, M. McGonigal, and S. T. Ceyer

Department of Chemistry, Massachusetts Institute of Technology, Cambridge, Massachusetts 02139

(Received 8 July 1994)

Abstraction of a F atom from incident F_2 by Si(100)-(2 × 1) is demonstrated by detection of the scattered, complementary F atom. He atom diffraction measurements are consistent with abstraction occurring at dangling bond sites. The low probability for single atom adsorption ($P_1 = 0.10 \pm 0.01$) relative to the total adsorption probability ($P_t = 0.96 \pm 0.02$) in the zero coverage limit indicates that the second F atom can also be trapped by the dangling bonds. Both the single and two atom adsorption probabilities decay to zero when the dangling bonds are saturated at 1 ML coverage. Atom abstraction represents a mechanism distinct from the classic one for dissociative chemisorption.

PACS numbers: 82.65.Pa, 34.50.Bw

One important function of a surface in heterogeneous catalysis or chemical vapor deposition is to cleave a bond of an incident molecule, thus forming two adsorbed reactive fragments. The dissociation proceeds by the formation of two bonds to the surface because the formation of two bonds is energetically necessary for bond cleavage. This is the classic view of dissociative chemisorption [1], and indeed this mechanism is operative in many molecule-surface systems. In contrast, one can envision bond cleavage by formation of a single surface-atom bond if the energy released by this bond formation is greater than the bond energy of the incident molecule. Generically, this mechanism is known as abstraction and is a well-documented reaction mechanism between two molecules in the gas phase. In this Letter, we document the dissociative chemisorption of a molecule on a surface by an abstraction mechanism. Specifically, we demonstrate that a Si(100)-(2 × 1) surface abstracts one F atom from an incident F_2 molecule by detecting the complementary F atom scattered back into the gas phase with a triply differentially pumped, rotatable, quadrupole mass spectrometer in a molecular-beam–surface-scattering UHV apparatus. In addition, we couple these experiments with He atom diffraction from the resulting fluorinated surface to demonstrate that the Si surface dangling bonds are responsible for the abstraction and are the sites for F adsorption. Because of the experimental complexities in the detection of reactive radicals such as F atoms, this mechanism has gone undetected in numerous previous studies of the interaction of fluorine and fluorine containing molecules with Si.

The apparatus has been described in detail [2]. The triply differentially pumped F_2 beam is formed by expansion of a mixture of 1% F_2 in Kr. The velocities of the incident and scattered beams are determined by cross correlation time-of-flight (TOF) methods. The beam is directed at an n-type Si(100) crystal that can be heated resistively and cooled to 120 K. The crystal is etched [3] prior to insertion into the vacuum chamber where it is repetitively sputtered and annealed (1120 K for 30 min) until Auger spectroscopy reveals carbon as the only contaminant, at a 1% or less level. He atom diffraction measurements show the surface to exhibit the well-documented (2 × 1) reconstruction associated with the formation of Si surface dimers. In real space, the surface exhibits rows of Si-Si dimers, with one dangling bond per Si atom.

Identification of the abstraction mechanism by detection of the scattered F atom is complicated by the fragmentation of the unreactively scattered F_2 in the electron bombardment ionizer of the mass spectrometer to produce both F_2^+ ($m/e = 38$) and F^+ ($m/e = 19$) ions. For example, a cracking ratio of $F^+/F_2^+ = 0.26$ is measured at 70 eV electron energy and a mass spectrometer 19 : 38 transmission ratio of 1. Therefore, the signal observed at $m/e = 19$ will contain a contribution from scattered F_2 as well as from F atoms, if present. We can distinguish between F^+ arising from F atoms and that produced by the cracking of F_2 on the basis of the different velocities with which they scatter from the surface. Figure 1(a) shows the TOF spectrum measured at $m/e = 19$. Two features are clearly observed in this spectrum, a narrow one at short times and a broad feature at longer times. Superimposed on this spectrum is the TOF distribution measured at $m/e = 38$, scaled by the F^+/F_2^+ cracking ratio. The single feature in this distribution occurs at the same flight time as the broad one in the $m/e = 19$ distribution and its intensity, scaled to represent the component of the $m/e = 19$ signal attributed to F_2, matches well the intensity of the broad feature in the $m/e = 19$ spectrum. These two observations lead to the conclusion that the broad feature arises from the cracking of the unreactively scattered F_2 while the narrow, short time feature arises from scattered F atoms. A point-by-point subtraction of the two distributions yields the net scattered F atom TOF distribution shown in Fig. 1(b). The solid lines are fits to these

 © 1995 The American Physical Society

distributions, as described in the figure captions. From these fits, the flux-weighted average velocities of F and F_2 are determined to be 1125 ± 100 and 422 ± 32 m/s, respectively, for a surface temperature of 250 K. The incident F_2 velocity is 390 m/s ($\Delta v = 50$ m/s). Measurements of the TOF distributions of F and F_2 scattered from a 1000 K surface show that the velocity of scattered F is independent of temperature (1181 ± 64 m/s) while the velocity of scattered F_2 is higher (607 ± 42 m/s). No ions are observed to desorb.

Additional confirmation of the presence of scattered F atoms comes from the F_2 exposure dependence of the scattered signal at $m/e = 19$ and 38 shown in Fig. 2(a). The signal at $m/e = 38$ is scaled by the $F^+/F_2{}^+$ cracking ratio so that it represents the component of the $m/e = 19$ signal that arises from F_2. The two signals have a very different dependence on F_2 exposure. While both signals become constant at high exposure, the $m/e = 19$ signal rises significantly more rapidly at very low exposure than the $m/e = 38$ signal. Point-by-point subtraction of the two plots yields the net $m/e = 19$ signal, shown in Fig. 2(b). It is clear that the F^+ signal at low exposure arises from a source different from the cracking of F_2 in the ionizer. We assign it to F atoms scattered from the surface. The F atom signal is a maximum at a low but nonzero exposure and then decays to zero with increasing exposure.

To probe the site of F adsorption, we measured He diffraction spectra from the clean and F-covered Si(100)-(2 × 1) surface. They are recorded by directing a supersonic He atom beam ($E = 11$ meV, $\Delta E = 4$ meV), incident on the 250 K surface 20° away from the normal angle, and then detecting the scattered He in 0.5° increments. The He beam is modulated at 150 Hz for the purpose of background subtraction. The diffraction spectra from a clean surface and a surface saturated with a F monolayer, showing the zero, half, and first order beams, are presented in Figs. 3(a) and 3(b), respectively. The key result is that the half order diffraction beam, which is the signature for the presence of the Si-Si dimers, is clearly present in the spectrum from the fluorinated surface, indicating that the adsorption of F does not break the dimer bond. Moreover, the diffraction intensities from the fluorinated surface [Fig. 3(b)] remain unchanged upon further F_2 exposure, indicating that the surface is saturated and that the F is adsorbed as an ordered overlayer with a (2 × 1) unit cell. In addition, we determined, as discussed below, that the coverage of this (2 × 1) overlayer is about 1 ML (one monolayer) which is equivalent to one F for every Si dangling bond. These observations are consistent with the reaction of F_2 with Si(100) occurring at the dangling bond sites of the surface dimers and adsorbing there, leaving Si-Si dimer bonds intact. This structural determination does not suffer from the ambiguity in LEED generated by efficient electron stimulated desorption of F [4] and is consistent with other results that identify SiF as the dominant species [5–8].

These results signal the observation of a new mechanism for dissociative chemisorption, atom abstraction. As F_2 is incident on this surface, a Si dangling bond abstracts one of the F atoms while the other F atom is scattered away. The cleavage of the F_2 bond by the formation of a single F-Si bond is thermodynamically feasible because the energy released upon adsorption on a single Si dangling bond, which does not require cleavage of a Si lattice bond, is 5–6 eV compared to 1.5 eV for the F_2 bond

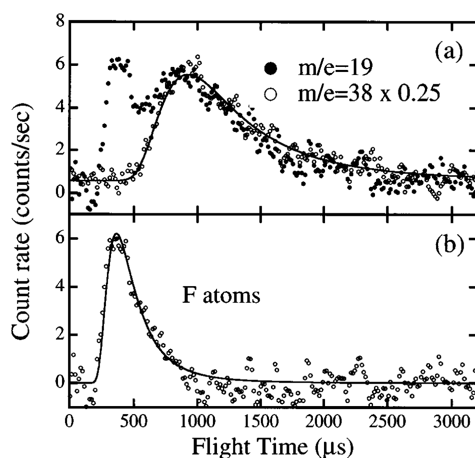

FIG. 1. (a) TOF at $m/e = 19$ and $m/e = 38$ multiplied by 0.25, cracking ratio of F_2, recorded at normal incidence ($\theta_i = 0°$) and at scattering angle $\theta_d = 35°$ away from normal angle. Spectra are averaged over F coverage from 0 to ~1 ML. Solid lines represent least squares fits of the function $At^{-4} \exp\{-(m/2kT_b)(l/t - v_f)^2\}$; t is flight time, l is flight length = 28.7 cm, m is mass, T_b is beam temperature, and v_f is flow velocity. (b) Net scattered F obtained by point-by-point subtraction of the $m/e = 19$ and 38 distributions in (a).

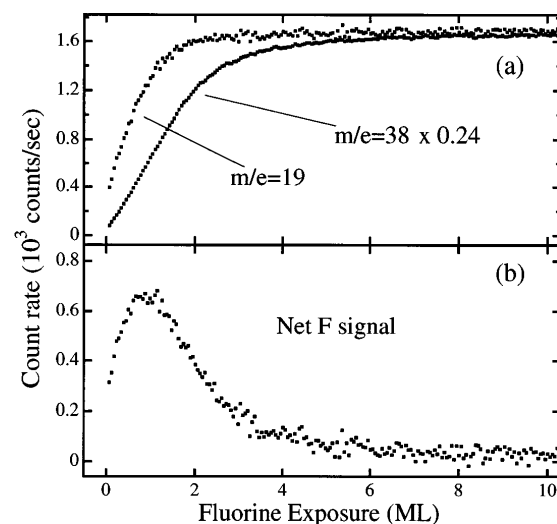

FIG. 2. (a) Signal at $m/e = 19$ and 38 (scaled by 0.25) recorded at $\theta_i = 0°$ and $\theta_d = 35°$ versus F_2 exposure in ML. A ML is equivalent to one F atom per Si atom. (b) Net F signal calculated by point-by-point subtraction of plots in (a).

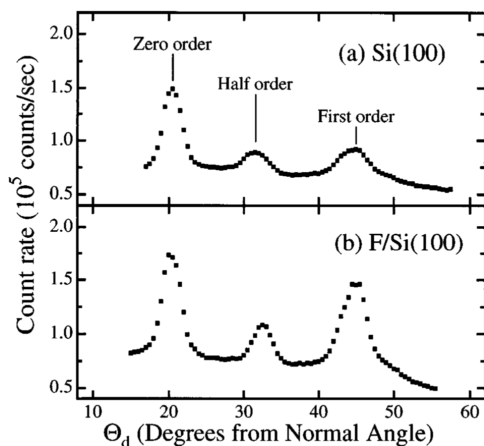

FIG. 3. He diffraction spectra from (a) Si(100)-(2 × 1), (b) 1 ML of F on Si(100) for $T_s = 250$ K, and $\theta_i = 20°$, $\lambda_{He} = 1.33$ Å. The He beam is incident along both the (10) and (01) azimuths because the surface is comprised of two orthogonal domains.

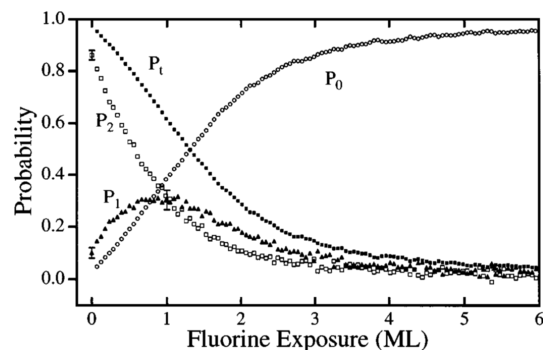

FIG. 4. Adsorption probability of a single F atom, P_1; both F atoms, P_2; total, P_t; and probability of no adsorption P_0 versus F_2 exposure for $T_s = 250$ K and $\theta_i = 0°$. Error bars are 95% confidence limits of five measurements carried out over 2 yr on four different crystals.

energy. Some of the exothermicity of this bond formation is converted into translational energy of the scattered F, as evident from the large velocity of the scattered F compared to the incident F_2 and the independence of the velocity on surface temperature. Abstraction has been observed in simulations of this system [9,10].

While the F atom that is not abstracted can scatter back into the gas phase, it does not necessarily do so. It may be caught on its outgoing trajectory by an adjacent dangling bond and adsorb there. It is also possible for both atoms to be simultaneously abstracted by two nearest neighbor dangling bonds if the F_2 molecular axis is favorably aligned upon its initial collision. We demonstrate that adsorption of both atoms also occurs by measuring the difference between the total F_2 adsorption probability P_t, and the probability for single atom adsorption P_1. P_t is determined from $1 - P_0$, where P_0, the probability for unreacted F_2 to be scattered from the surface, is the ratio of the angle integrated F_2 flux to the incident F_2 flux. P_1 is the ratio of the angle integrated F flux to the incident F_2 flux. The difference $P_t - P_1$ is the probability for adsorption of both F atoms, P_2, and is plotted in Fig. 4, along with P_1 and P_t, versus exposure. The coverage, which may be determined by integrating $P_2 + 0.5P_1$ over F_2 exposure, approaches approximately 1 ML at P_t decays toward zero and as the dangling bonds saturate. In the zero coverage limit, P_2 contributes 0.86 ± 0.02 and P_1 contributes 0.10 ± 0.01 to the total P_t of 0.96 ± 0.02, in reasonable agreement with simulations [9,10] and with a previous experimental result [11] for P_t.

The maximum in P_1 at a nonzero coverage is also consistent with the presence of a reaction channel in which both F atoms are adsorbed. P_1 is small in the limit of zero coverage, because the dangling bonds adjacent to the abstraction site of the first F atom are likely unoccupied and, therefore, have a high probability of trapping the second F. As the coverage increases, the probability of having unoccupied adjacent sites decreases, thereby leading to a higher probability that the second F does not adsorb but scatters back to the gas phase. As the coverage increases yet further, the effect of the diminishing number of sites for abstraction of the initial F dominates, leading to an overall decay of P_1. In short, the maximum in P_1 arises from the competition between the number of abstraction sites available to the incident F_2, which decreases with coverage, and the number of occupied sites (which cannot trap the second F) adjacent to the abstraction site, which increases with coverage. A simple analytical model that incorporates these physical features reproduces these data and will be presented in a future publication. Note that P_1 is a lower limit to the abstraction probability because its value is based only on those complementary atoms which successfully scatter back to the gas phase.

We have identified and characterized a new mechanism for dissociative chemisorption, atom abstraction. This mechanism is a consequence of the high exothermicity of the reaction between F_2 and Si and should be observable in and is suggested by data from other exothermic molecule-surface interactions [12–14]. This mechanism may also be an additional source of radicals that have been previously unaccounted for in models for plasma etching. Recently, evidence for the reverse of this process has been presented [15,16].

This work is supported by JSEP Grant No. DAAL03-92-C-0001 and NSF Grant No. CHE-9318636.

[1] R. P. H. Gasser, *An Introduction to Chemisorption and Catalysis by Metals* (Oxford University Press, New York, 1985), p. 5.

[2] S. T. Ceyer, D. J. Gladstone, M. McGonigal, and M. T. Schulberg, *Physical Methods of Chemistry,* edited by B. W. Rossiter and R. C. Baetzold (Wiley, New York, 1993), 2nd ed., Vol. IXA, p. 383.

[3] A. Ishizaka and Y. Shiraki, J. Electrochem. Soc. **133**, 666 (1986).

[4] N. D. Shinn, J. F. Morar, and F. R. McFeely, J. Vac. Sci. Technol. A **2**, 1593 (1984).

[5] M. J. Bozack, M. J. Dresser, W. J. Choyke, P. A. Taylor, and J. T. Yates, Jr., Surf. Sci. **184**, L332 (1987).

[6] F. R. McFeely, J. F. Morar, N. D. Shinn, G. Landgren, and F. J. Himpsel, Phys. Rev. B **30**, 764 (1984).

[7] C. J. Wu and E. A. Carter, Phys. Rev. B **45**, 9065 (1992).

[8] T. A. Schoolcraft and B. J. Garrison, J. Vac. Sci. Technol. A **8**, 3496 (1990).

[9] T. A. Weber and F. H. Stillinger, J. Chem. Phys. **92**, 6239 (1990).

[10] L. E. Carter, S. Khodabandeh, P. C. Weakliem, and E. A. Carter, J. Chem. Phys. **100**, 2277 (1994).

[11] J. R. Engstrom, M. M. Nelson, and T. Engel, Surf. Sci. **215**, 437 (1989).

[12] D. J. Driscoll, W. Martir, J. X. Wang, and J. H. Lunsford, J. Am. Chem. Soc. **107**, 58 (1985).

[13] J. T. Roberts and C. M. Friend, Surf. Sci. **202**, 405 (1988).

[14] J. L. Lin and B. E. Bent, J. Am. Chem. Soc. **115**, 2849 (1993).

[15] E. W. Kuipers, A. Vardi, A. Danon, and A. Amirav, Phys. Rev. Lett. **66**, 116 (1991).

[16] C. T. Rettner, Phys. Rev. Lett. **69**, 383 (1992).